Fibers and Polymers 2017, Vol.18, No.7, 1288-1295
DOI 10.1007/s12221-017-7123-x

ISSN 1229-9197 (print version)
ISSN 1875-0052 (electronic version)

Mechanical and Moisture Absorption Characterization of PLA Composites Reinforced with Nano-coated Flax Fibers

Marie Bayart, Florent Gauvin, M. Reza Foruzanmehr, Saïd Elkoun, and Mathieu Robert*

Carrefour of Innovative Technology and Ecodesign, University of Sherbrooke, Quebec J1K 2R1, Canada

(Received February 14, 2017; Revised April 27, 2017; Accepted April 30, 2017)

Abstract: This research is intended to improve the interface between the fibers and the matrix and limit water absorption of bio-based material thereby decreasing degradation of the composites when they are exposed to external environment such as high temperature and humidity. In this study, flax fibers were treated with an organic surface coating containing SiO_2 nanoparticles. This coating was a dispersion of silica fume in epoxy. One composite was also made with raw fibers as reference as well as one sample of pure PLA. Flax fibers/PLA composites were manufactured by hot pressing by stacking 4 PLA films and 3 pieces of flax fabric. Morphology and dispersion of the coating on the fibers was observed by scanning electron microscopy (SEM), small-angle X-ray scattering (SAXS) and transmission electron microscopy (TEM). Accelerated ageing was carried out on the 3 materials by placing them in a 50 °C water bath until saturation to investigate the influence of the coating on water diffusion. Mechanical properties of the different composites were investigated by tensile (before and after conditioning) and short beam shear (SBS) testing in order to evaluate the impact of the coating on the interfacial properties of the materials. The results show that the fibers surface was homogenized and that a better adhesion was reached because of the coating. Coating the fibers also allowed the decrease in water uptake by more than 10 % and their protection during conditioning, preserving their mechanical properties.

Keywords: Natural fibers coating, Polylactic acid, Green composites, Interface, Water absorption

Introduction

Nowadays, research, development and production of environmentally friendly materials are growing. Many studies deal with the creation of greener materials in order to reduce greenhouse gas emission during processing, use and end of life [1-4]. The automotive industry already produces composites containing natural fibers for cars interiors such as doors and hood panels [5]. The matrix is generally polypropylene (PP) while kenaf, jute or flax fibers are commonly used as reinforcements [6-8].

In Canada, around 800,000 hectares of flax are produced annually to collect seeds. However, stems containing the fibers are either thrown away or burnt. Using these natural fibers could be a great way to valorize agriculture waste. With this in mind, natural fibers and especially flax fibers have been highly investigated as reinforcements for composite materials [9]. They have excellent mechanical properties and could be a good replacement to mostly used synthetic fibers such as glass [10].

Vegetal (cellulosic) natural fibers are renewable, biodegradable and nontoxic materials. They are extracted from different sources such as shells, fruits, stems and leaves. They can be considered as composites themselves because of their composition that incorporates semi-crystalline cellulose (71 % in flax, 72 % in kenaf, 61-71 % in jute [11]) in an amorphous matrix of hemicelluloses and lignin. Cellulose microfibrils are helically wound along the fiber axis to form ultimate hollow cells [12], explaining a low density and a high specific strength [13]. The central tube is also known as lumen, permitting water delivery by capillary action.

However, natural fibers (NF) have two major drawbacks, affecting their dispersion and the interface between them and the matrix. The first issue is the low adherence between cellulosic fibers and polymer matrices. Natural fibers usually contain more than 70 % of hydrophilic cellulose, making their surface highly polar because of their many -OH groups, resulting in a poor interfacial bonding with polymer matrices. A weak interface between the matrix and the fibers is shown in Bax and Müssig study resulting from this issue [14]. The SEM pictures of the fracture surfaces of their impact specimens show pulled out fibers and holes, highlighting the poor adhesion.

The second major drawback of natural fibers is their high hydrophilicity due to their hollow structure and their cell wall containing hydrophilic cellulose, as said previously [15]. This drawback affects inevitably the NF-reinforced composites. The gap between the matrix and the fiber is also a cause of water uptake [16]. Water absorption can induce swelling of the material which may generate cracks in the matrix. Islam *et al*. have conducted a study based on accelerated ageing in 50 °C water of polylactic acid (PLA)/ hemp composites [17]. They concluded that fibers were the main cause of water absorption. Consequently, mechanical properties of the composites were drastically reduced. Joseph *et al*. found that increasing the water temperature up to 70 °C increased the water sorption [18]. These are serious issues for long-term applications where composites may be exposed to similar humidity and temperature conditions.

As a consequence, it is crucial to modify the matrix or/and

*Corresponding author: Mathieu.Robert2@USherbrooke.ca

the fibers surface to avoid these phenomena. Several chemical treatments react with the hydroxyl groups present on cellulose surface and therefore, reduce their hydrophilicity [19]. Mercerization decreases fibers surface roughness by dissolving certain components as waxes and lignin and enhances cellulose crystals exposition [20]. Physical treatments like plasma or corona help cleaning the fibers surface, removing some materials of it, and functionalizing them [21].

All these treatments improve the interface between the matrix and the fibers but some issues remain such as their tendency to absorb water [22].

Another possibility to modify the fibers surface is to coat them. Coating enables a good smoothing of the fibers surface by filling the imperfections and makes the fibers more homogeneous. Foruzanmehr *et al*. functionalized flax fibers by coating them with TiO_2. They observed a good interface between the fibers and the coating and a significant increase in the fibers mechanical properties [23]. They discovered that oxidizing the cellulosic fibers prior to the sol-gel coating improved its quality [24]. Nano-reinforced coating is also an important topic of research. Indeed, nanoparticles present in the coating prevent from crack initiation, generally induced by imperfections. They increase the coating rigidity as well as those of the fibers. Nanoparticles also limit water permeability in the composite, which could avoid fibers swelling, hydrolysis and thus defects in the materials [25,26]. Gauvin *et al*. used a dispersion of modified SiO_2 nanoparticles in an epoxy matrix to coat bamboo fibers. They obtained a better interface leading to a significant increase in the mechanical properties of the composites up to 28 % [27].

Finally, natural fibers degrade at high temperatures, which limits the processing temperature to 200 °C [28]. Consequently, the matrix needs to have a low melting point.

The main goal in the development of environmentally friendly composites is to produce totally green composites, namely natural fibers within a biopolymer matrix.

Polylactic acid (PLA), polyglycolic acid (PGA) and polyhydroxyl butyrate (PHB) are biodegradable biopolymers extracted from biomass such as vegetables containing starch and sugar-crops. Their processing and use show a lower carbon footprint than petroleum based polymers [29]. Their mechanical properties are comparable to commonly used petroleum based polymers like PP. Among these bioplastics, PLA distinguishes itself with its low melting temperature around 160 °C, preventing fibers from degradation, and its industrial availability. In addition, it is probable that hydrophilic nature of PLA could enable a better compatibility with hydrophilic fibers. However, PLA is highly brittle and has the lowest ductility among petroleum based polymers. Researchers have tried to improve PLA properties by adding plasticizers. This decreased PLA stiffness and so its brittleness. It also helped PLA to exhibit higher elongations [30]. Adding reinforcement to the matrix is also a good way to increase PLA properties. Natural fibers can be added to PLA in order to improve impact resistance. Foruzanmehr *et al.* reinforced PLA with TiO_2 grafted flax fibers and obtained a three time-increase in impact resistance [31]. Oksman *et al*. compounded flax fibers to PLA and found that the composite strength was about 50 % higher than a similar PP/flax composite but concluded that improving the interface between the fibers and the matrix would increase even more the composite properties [32].

The aim of this study was to investigate the efficiency of a flax fibers coating treatment before processing green flax/PLA composites. The elaborated composites might have semi-structural applications such as interior cladding, siding and sheathing in building engineering and interior trimming for car industry. Thin film coatings are usually used to fill the fibers defects and to reduce their surface polarity to create stronger bonds with the polymeric matrix. A treatment consisting in a dispersion of colloidal silica fume in epoxy was investigated. Even though the epoxy matrix used in this study was not green, the coating was so thin that it was negligible compared to the amount of the other green materials used. Hydroxyl groups present along the chains of epoxy resins enable strong bonds to hydroxyl surfaces such as natural fibers surfaces. This polymer also has a lower surface energy than natural fibers and permits to decrease their polarity and thus, a better adhesion to PLA. Coating the fibers with epoxy should also prevent them from absorbing water. Nanoparticles of silica could also inhibit the crack propagation in the composites and water absorption. Three types of materials, two composites with coated and raw fibers and pure PLA, were processed by thermal compression. Tensile and Short Beam Shear (SBS) tests were carried out to measure the influence of the treatment on the composites mechanical and interfacial properties. Fractured surface of composites were observed with a Scanning Electron Microscope (SEM) to study the rupture mechanisms and correlate them to the quality of the interface. Samples were immerged in a water bath at 50 °C to measure water diffusion through raw fiber composites (RF-C), Nanopox-coated fiber composites (NCF-C) and pure PLA.

Experimental

Materials

Technical fibers and unidirectional fabric were supplied by Procotex (Belgium) and FRD, Fibres Recherches Développement (France) respectively. The average diameter of the fibers was approximately 10 μm according to optical microscopy. PLA 4032D pellets were supplied by NatureWorks LLC. The SiO_2/epoxy suspension called Nanopox F400 was supplied by Evonik Industries. Nanopox consists of 5 % of colloidal silica fume with approximately 20 nm diameter.

Coating of the Flax Fibers and Fabrics

Flax fibers and fabrics were dried at 50 °C overnight in order to remove all residual moisture. Nanopox was diluted in a large volume of acetone (1:50 weight ratio). Then, flax fibers and fabrics were dip-coated in the solution 10 times backward and forward (approximately during one minute). Remaining acetone was evaporated at room temperature, leading to the formation of a thin film on the fibers surface (Figure 4). Raw flax fibers and fabrics (RF) were also used to compare their surface with the Nanopox-coated fibers and fabrics (NCF) and to make the third composite.

Composites Processing

Unidirectional RF-C and NCF-C were processed by alternating 4 thin plies of PLA and 3 plies of flax fabric oriented at 0 °, in accordance with Figure 1. All the samples were hot pressed at 180 °C following the next pressure cycle: 5 minutes at 0 Tons (T), 1.5 minutes at 2 T, 1 minute at 1 T, 30 seconds at 0.5 T and 10 seconds at 6 T.

Resulting molded composites were 2 mm thick and contained approximately 30 % of fibers by weight. The relative density of the composites, according to ASTM D792, was 1.15 g/cm^3 and 1.185 g/cm^3 for the RF-C and NCF-C respectively.

The void content of the composites, according to ASTM D2734, was 13.5 % and 10.9 % for the RF-C and NCF-C respectively. The Nanopox coating decreased the void content by filling the defects and lumen of the fibers.

Scanning Electron Microscope (SEM)

In order to characterize the morphology of the RF and NCF surface, SEM analyses were performed using a Hitachi S-3000N with the secondary electron (SE) mode at 5 kV. Single fibers were observed to compare the quality of their surface and the differences between RF and NCF. Fractured samples after SBS tests were also investigated. All specimens were sputtered with a thin layer of gold-platinum before analysis.

Small Angle X-ray Scattering (SAXS)

SAXS analyses were carried out in order to confirm the size of the SiO_2 nanoparticles in the Nanopox resin. The SAXS patterns were collected with a Bruker AXS Nanostar system equipped with a Microfocus Copper Anode at 50 kV/ 0.60 mA, MONTAL OPTICS and a VANTEC 2000 2D detector at 1086.000 mm distance from the samples calibrated with a Silver Behenate standard. The diffracted intensities were then integrated from 0.10 to 3.00 deg. 2-theta and treated with Primus GNOM 3.0 program from ATSAS 2.3 softwares, to determine the particle sizes by pair distance distribution [33]. The collection exposure times were 1000 seconds/sample. NCF were also observed to verify the presence of the coating on their surface and to characterize the homogeneity of the coating in terms of particles dispersion.

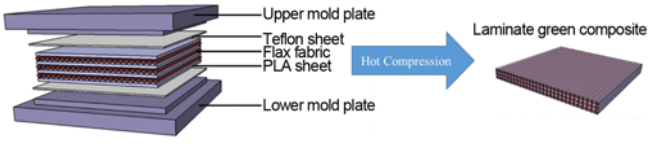

Figure 1. Laminate green composite processing.

Transmission Electron Microscope (TEM)

Transversal sections of the coated fibers were examined on a copper grid with a Hitachi H-7500 transmission electron microscope at 80 kV. They were cut at a thickness of 80 nm with a diamond knife on an ultramicrotome.

Tensile Properties of Composites

Tensile tests were carried out according to ASTM D3039 standard (following the specimen geometry recommendation with a dimension of 120×25×2 mm) using a Zwick/Roell z050 testing machine equipped with a 30 kN load cell and a Zwick multiXtens Extensometer. The tests were conducted by controlling the displacement using a crosshead speed of 2 mm/min. The Young modulus (E) and Ultimate tensile strength (UTS) of Fiber Reinforced Polymer (FRP) were determined. More than five specimens of each composition were tested.

Short Beam Shear (SBS) Testing of Composites

SBS tests were performed on the composites according to ASTM D2344 standard to determine their interlaminar shear strength (ILSS). The span-to-thickness ratio was set at 4:1. All the tests were conducted on Zwick/Roell z050 testing machine equipped with a 30 kN load cell. The crosshead speed was 1 mm/min. More than five specimens for each sample were tested. The ILSS was calculated according to equation (1):

$$ILSS = \frac{3}{4}\frac{P_m}{bd} \quad (1)$$

where ILSS is the maximum interlaminar shear strength, P_m is the maximum applied load, and b and d are the width and the thickness of the specimens respectively.

Water Absorption

Water absorption measurements were performed according to ASTM D570 by immersing FRP and pure PLA in deionized water at 50 °C. Specimens were shaped as 20×30× 2 mm, with an approximate weight from 1.4 to 1.7 g. They were dried until they reached a constant mass with a precision of 0.1 mg and were then put in separated distilled water bath at 50 °C. Sides oriented along the x and y axis and edges were covered with hydrophobic paint to concentrate water diffusion along the z axis (Figure 2).

Five specimens for each sample were periodically removed

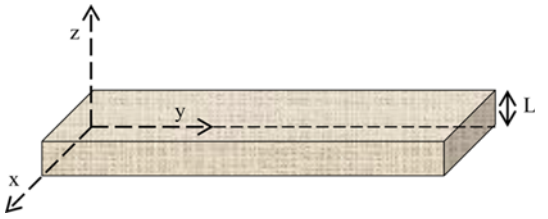

Figure 2. Test specimen geometry in Cartesian system.

from water, dried and weighed immediately, until they reached full saturation. Water uptake was calculated using equation (2), where *%M* is the mass gain due to moisture uptake, M_{cond} the mass after conditioning and M_{dry} the mass before conditioning.

$$\%M = \frac{100 \times (M_{cond} - M_{dry})}{M_{dry}} \quad (2)$$

By following the Fick's theory of diffusion, coefficient of diffusion was calculated by plotting the mass gain as a function of time. At short times, Fick's law is given as equation (3) where *D* is the coefficient of diffusion, *L* the thickness, *t* the time, M_t the percentage of absorbed water at time t, and M_∞ the mass gain at equilibrium [34].

$$D = \left(\frac{L}{4} \times \frac{M_t}{M_\infty}\right)^2 \times \frac{\pi}{t} \quad (3)$$

Results and Discussion

Microstructural Analysis of Fibers and Their Coating

SEM analyzes were performed on RF and NCF. Figure 3 shows a single fiber for each condition: a) RF; b) NCF.

Defects are noticeable on the RF surface and it is neither smooth nor homogeneous. However, for the NCF, imperfections are covered up and voids are filled, giving the fiber a uniform surface.

In order to investigate the interface quality between the fiber and its coating, TEM observations were carried out and results were shown in Figure 4.

Picture a) highlights that the particles size is constant and that their dispersion in the epoxy resin is good. Thus, the coating should be homogeneous. Picture b) confirms this hypothesis by showing that NCF were coated with a thin homogeneous film containing SiO_2 nanoparticles and that the interface between the fibers and the coating is cleared from defects and voids.

Dispersion and Size of the Nanoparticles

In this study, it was more relevant to interpret the structural properties analyzing the pair distribution functions rather than the scattering data themselves [35]. SAXS pair distribution functions (Figure 5) permitted to verify the size of the nanoparticles present in the epoxy coating and the dispersion of the nanoparticles in the coating, when it was

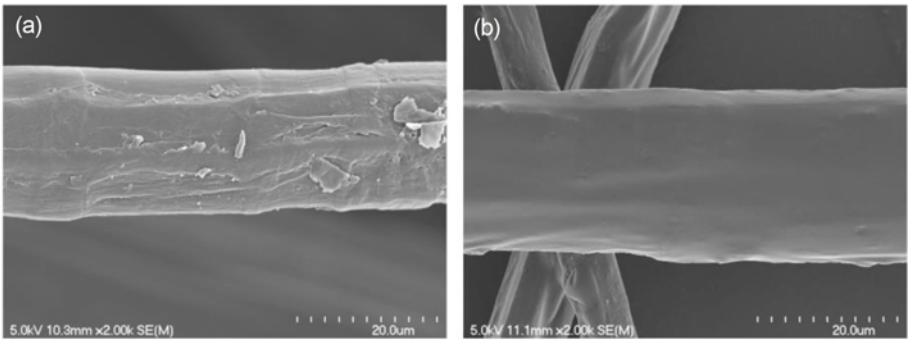

Figure 3. SEM observation of (a) RF and (b) NCF.

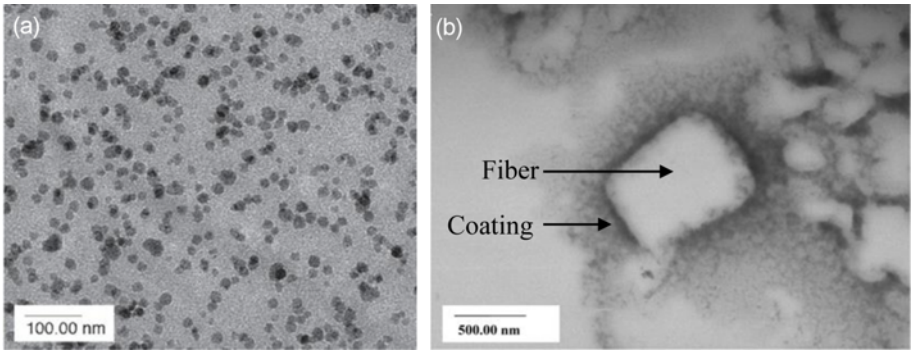

Figure 4. TEM observation of (a) Nanopox and (b) NCF.

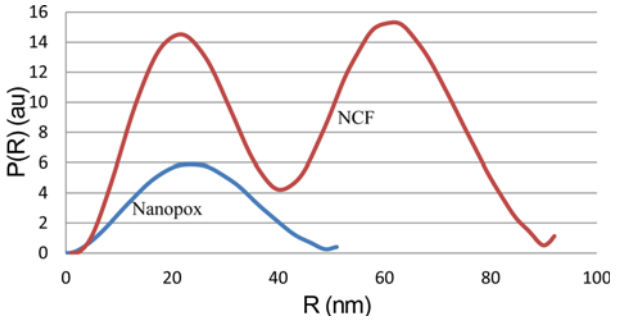

Figure 5. SAXS pair distribution functions of a Solution of Nanopox diluted in acetone 1:150 and a NCF.

applied on the surface of the fibers.

The Gaussian curve of Nanopox diluted in acetone, typical in case of spherical particles, reaches a maximum at an abscissa of 24 nm, giving the average SiO_2 particles size. The pair distribution function of NCF is a double Gaussian curve suggesting a dumbbell-shaped particle or two particles with a very small inter-particle distance [36]. This difference on NCF means that particles were regularly distributed very close to each other in the coating applied on the surface of the fibers but not overlapped. This is the result of a good dispersion and it legitimizes the dip coating method used.

Mechanical Characterization of the Composites before Conditioning

As seen in Table 1, the tensile modulus and the ultimate tensile strength (UTS) of the pure PLA resin were found to be 2.09 GPa and 59.8 MPa respectively. Concerning the composites, they were found to be respectively 10.8 GPa and 177 MPa for the RF-C and 12.2 GPa and 187 MPa for the NCF-C. The coating permitted to increase the composites tensile modulus and thus their rigidity by 13 % and their UTS by 6 %. The tensile modulus of coated samples increased by filling the fibers defects and voids, and increasing the interface quality. Nanoparticles also participated in this increase by restraining the chains mobility of the fibers. As nanoparticles made the coating more rigid, they must also have been a reason of this increase. The UTS did not show a significant increase. Indeed, as the cellulose micro-fibrils were not able to move anymore and align in the tensile direction, stress concentration appeared and thus, a premature rupture [37].

Nevertheless, as it was seen in the SEM pictures of the RF and NCF, the coating permitted to blunt the defects on the surface of the fibers and certainly prevented cracks from initiating and stress to concentrate in these previously defective zones, this reason might be the explanation for the 6 % increase in the UTS of the coated samples.

Concerning the rupture mechanisms, it can be noticed that for both the composites, the elongation at break drastically dropped. This can be related to the cellulose micro-fibrils, whose mobility was reduced by the matrix. Elongation at break was even more decreased for the NCF-C. Indeed, nanoparticles can entangle in the matrix chains and in the cellulose micro-fibrils and prevent them from aligning in the tensile direction during solicitation. Thus, the composites have a fragile behavior whereas pure PLA was ductile [38].

The SBS tests were performed to determine the ILSS of the different composites in order to investigate whether the coating improved the interfacial adhesion of the treated composites or not.

Results of the influence of the coating on the ILSS of the composites are given in Table 1. The obtained value for the ILSS of the RF-C was 20.58 MPa compared to 24.84 MPa for the NCF-C. This corresponds to an increase of 20.7 %. These values proved that a better adhesion was achieved between the flax fibers and the PLA matrix when the fibers were coated with Nanopox. When they are submitted to shear, the different layers of laminate composites tend to delaminate to release energy. A good interfacial adhesion provides a good load transfer, delays this phenomenon and thus increases the maximal interlaminar shear strength.

Moreover, it is noticeable that the standard deviation of the SBS results decreased in the case of the NCF-C compared to the RF-C. This confirmed that the coating gave the composites a homogeneous surface and thus, consistent mechanical properties.

The combination of these results revealed that the coating did not reinforce the fibers themselves but their interface with the matrix in the composites.

Microstructural Analysis of the Fractured Composites Samples

The SEM observations shown in Figure 6 were performed on fractured composite samples after SBS. These permitted to investigate the quality of the interface between the NCF and the matrix in the NCF-C and to compare it to the RF-C.

It can be noticed that for the RF-C, the fibers did not adhere at all to the matrix and pulled out during the SBS test.

Table 1. Influence of the coating on the composites tensile and interfacial properties (before conditioning)

	RF-C				NCF-C				Pure PLA		
	E (GPa)	σ (MPa)	ε (%)	ILSS (MPa)	*E* (GPa)	σ (MPa)	ε (%)	ILSS (MPa)	E (GPa)	σ (MPa)	ε (%)
Average	10.8	177	1.7	20.58	12.2	187	1.6	24.84	2.09	59.8	5.8
SD	0.196	14	0.084	2.02	0.33	10.6	0.08	0.650	0.08	1.48	0.4

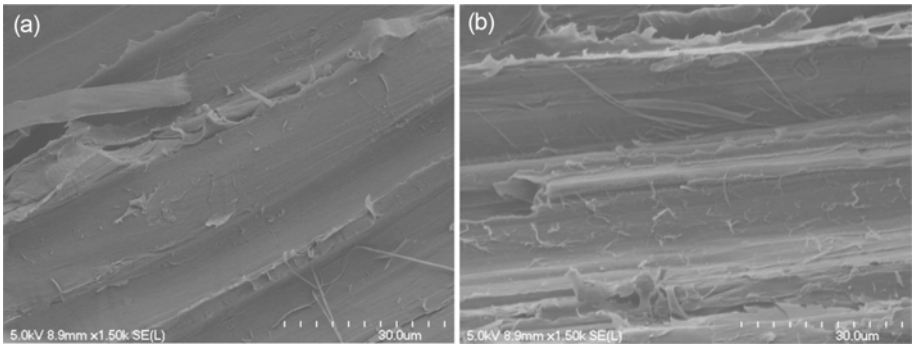

Figure 6. Microstructural analysis of the fractured samples; (a) RF-C and (b) NCF-C.

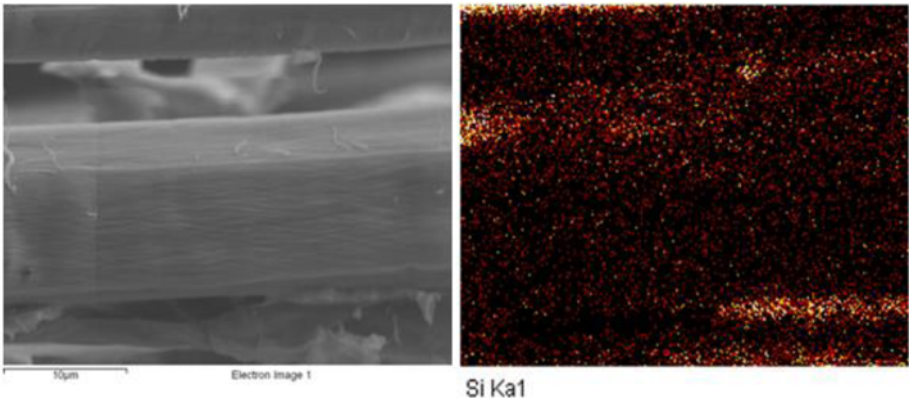

Figure 7. Mapping of a NCF after SBS test.

There are no significant traces of the fibers presence in picture a). However, for the NCF-C, it is clear that fibers did not pull out easily during the SBS test. There are fibrils remaining in the matrix, meaning that the coating improved the adhesion of the fibers on it. A mapping was also conducted on a NCF surface (Figure 7) which showed the existence of silicium on it. This proves that some coating remained on the fibers surface, meaning that the adhesion between the fibers and the coating was also strong.

Moisture Absorption of Composites

Figure 8 represents the percentage of water uptake as a function of time.

It is noticeable that the trend in water diffusion is the same at the beginning of the test for the two composite materials. Indeed, the curve slope is the same for these two cases, meaning that the rate of diffusion is the same for both composite samples despite the coating. The coefficient of diffusion was calculated according to equation (3) and was logically found to be the same in both of them (approximately 7.0×10^{-13} m^2s^{-1}). However, at the end of the test, after obtaining the plateau, meaning that the samples had reached water saturation, the difference of water absorption between the different samples was significant, showing a decrease of 10.3 % after treatment. This means that the coating filled the porosities and probably the fibers lumen [39], limiting the

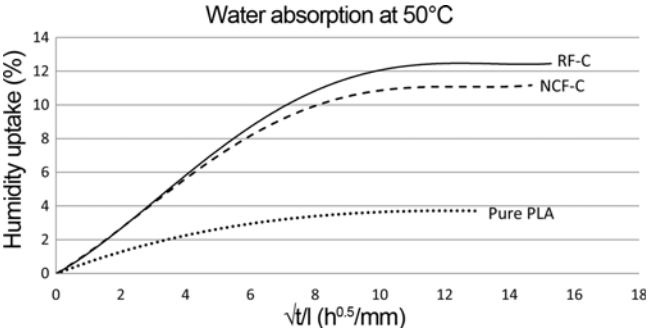

Figure 8. Water absorption at 50 °C of RF-C (full line); NCF-C (dashed line); and pure PLA (dotted line).

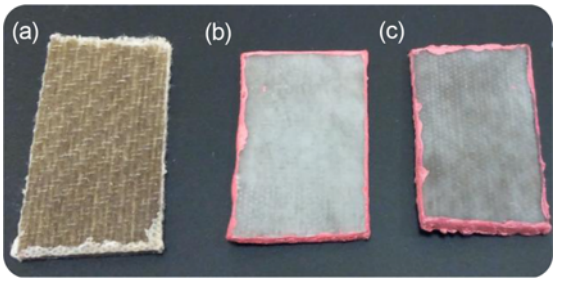

Figure 9. Surface macroscopical aspect of the composites; (a) before conditioning, (b) RF-C after conditioning, and (c) NCF-C after conditioning.

Table 2. Influence of the coating on the composites mechanical properties after conditioning

	RF-C			NCF-C		
	E (GPa)	σ (MPa)	ε (%)	E (GPa)	σ (MPa)	ε (%)
Average	4.68	89	5.2	6.2	114	4.8
SD	0.49	8.78	0.3	0.5	3.39	0.6

water amount at saturation. Water absorption in PLA was much lower than those in the other samples. This means that the fibers (RF and NCF) were the main cause of water absorption. Figure 9 shows the macroscopic aspect of the composites after conditioning.

It is noticeable that there was a significant degradation of the composites after the water absorption study compared to the composite sample before conditioning. Also, the residual water took a yellowish color that was stronger for the RF-C than for the NCF-C. Moreover, the RF-C seemed more degraded. They were whiter than the NCF-C. This may mean that the samples were degraded in hot water and some components of the fibers were dissolved. Indeed, some components can melt at low temperatures. It is the case of waxes [23]. This phenomenon was stronger for the RF-C than the NCF-C. The coating may have protected the NCF from a more serious degradation. In addition, water absorption in the different materials involved swelling. Pure PLA samples were subjected to a 2.7 % increase in their thickness. The presence of fibers induced a 14.9 % and a 19.2 % increase in the NCF-C and RF-C thickness respectively. Again, the coating avoided the NCF-C from swelling as much as the RF-C by filling the voids, defects and lumen of the fibers.

Mechanical Characterization of the Composites After Conditioning

Table 2 reveals the results of the tensile tests made on the composites after conditioning. These results confirm the hypothesis made in the previous section. Indeed, the coating protected the fibers. The Young's modulus of the NCF-C was found to be 6.2 GPa whereas it was 4.68 GPa for the RF-C. This equals to a 43.3 % retention rate for the RF-C and a 50.8 % retention rate for the NCF-C. The links between the fibrils must have been very degraded for the RF-C whereas they were protected by the coating for the NCF-C. Moreover, the UTS results were also significant. The UTS was found to be 114 MPa and 89 MPa for the NCF-C and RF-C respectively. This corresponds to a retention rate of 61 % for the NCF-C and of 50.3 % for the RF-C. Elongation at break increased in the two cases because of the degradation that made the fibrils more mobile. It was more important for the RF-C, revealing again a higher degradation.

Conclusion

This study focused on the influence of an epoxy coating containing dispersed silica fumes on the mechanical and interfacial properties, and water absorption of PLA/flax composites. According to this work, the following conclusions can be drawn:

1. The coating of the fibers led to a homogenization of their surface. This was revealed by SEM picture and tensile tests, where less stress concentration occurred, enhancing the tensile modulus of the composites up to 13 %. A better adhesion with the matrix was also noticed. Indeed, it was shown that the coating had a significant influence on the composites properties by enhancing their interlaminar shear strength up to more than 20 %.
2. The mass uptake at saturation for the RF-C and the NCF-C were 12.45 % and 11.17 % respectively, showing a decrease of 10.3 % after treatment. This decrease is linked to the filling and homogenization of the voids, defects and lumen of the fibers and to the better adhesion between the fibers and the PLA matrix, avoiding moisture absorption by the fiber/matrix interface.
3. The coating protected the fibers. Indeed, results of the mechanical properties after conditioning were significantly higher for the NCF-C than the RF-C (a 43.3 % and 50.8 % retention rate for the RF-C and NCF-C respectively for the Young's modulus and a 50.3 % and 61 % retention rate for the RF-C and NCF-C respectively for the UTS).

Finally, this research highlights the possibility to produce green composites with high mechanical properties and low water absorption, following a simple and efficient method of dip coating without any fibers pretreatment. This process could easily be industrialized and does not need the use of many chemicals, making it very cheap.

Acknowledgement

This research was supported by the National Science and Engineering Research Council (NSERC) of Canada and by the Consortium Innovation Polymères (CIP). The authors would like to thank Evonik Industries for providing the Nanopox resin.

References

1. L. L. Kosbar, J. D. Gelorme, R. M. Japp, and W. T. Fotorny, *J. Ind. Ecol.*, **4**, 93 (2000).
2. M. M. Davoodi, S. M. Sapuan, D. Ahmad, A. Ali, A. Khalina, and M. Jonoobi, *Mater. Des.*, **31**, 4927 (2010).
3. K. Petersen, P. V. Nielsen, and M. B. Olsen, *Starch - Stärke*, **53**, 356 (2001).
4. K. Petersen, P. V. Nielsen, G. Bertelsen, M. Lawther, M. B. Olsen, N. H. Nilsson, and G. Mortensen, *Trends Food Sci. Technol.*, **10**, 52 (1999).

5. J. Holbery and D. Houston, *JOM*, **58**, 80 (2006).
6. B. Dahlke, H. Larbig, H. D. Scherzer, and R. Poltrock, *J. Cell. Plast.*, **34**, 361 (1998).
7. Y. Chen, O. Chiparus, L. Sun, I. Negulescu, D. V. Parikh, and T. A. Calamari, *J. Ind. Text*., **35**, 47 (2005).
8. D. V. Parikh, T. A. Calamari, A. P. S. Sawhney, E. J. Blanchard, F. J. Screen, J. C. Myatt, D. H. Muller, and D. D. Stryjewski, *Text. Res. J.*, **72**, 668 (2002).
9. J. Andersons, E. Spārniņš, and R. Joffe, *Polym. Compos*., **27**, 221 (2006).
10. S. V. Joshi, L. T. Drzal, A. K. Mohanty, and S. Arora, *Compos. Pt. A-Appl. Sci. Manuf.*, **35**, 371 (2004).
11. M. J. John and R. D. Anandjiwala, *Polym. Compos*., **29**, 187 (2008).
12. M. Z. Rong, M. Q. Zhang, Y. Liu, G. C. Yang, and H. M. Zeng, *Compos. Sci. Technol*., **61**, 1437 (2001).
13. D. N. Saheb and J. P. Jog, *Adv. Polym. Technol*., **18**, 351 (1999).
14. B. Bax and J. Müssig, *Compos. Sci. Technol*., **68**, 1601 (2008).
15. Z. N. Azwa, B. F. Yousif, A. C. Manalo, and W. Karunasena, *Mater. Des*., **47**, 424 (2013).
16. A. C. Karmaker, *J. Mater. Sci. Lett*., **16**, 462 (1997).
17. M. S. Islam, K. L. Pickering, and N. J. Foreman, *Polym. Degrad. Stabil*., **95**, 59 (2010).
18. P. V. Joseph, M. S. Rabello, L. H. C. Mattoso, K. Joseph, and S. Thomas, *Compos. Sci. Technol*., **62**, 1357 (2002).
19. A. K. Bledzki, S. Reihmane, and J. Gassan, *J. Appl. Polym. Sci*., **59**, 1329 (1996).
20. A. K. Mohanty, M. Misra, and L. T. Drzal, *Compos. Interfaces*, **8**, 313 (2001).
21. S. Mukhopadhyay and R. Fangueiro, *J. Thermoplast. Compos. Mater*., **22**, 135 (2009).
22. S. Rizkalla, T. Hassan, and N. Hassan, *Prog. Struct. Eng. Mater.*, **5**, 16 (2003).
23. Mr. Foruzanmehr, P. Y. Vuillaume, M. Robert, and S. Elkoun, *Mater. Des*., **85**, 671 (2015).
24. Mr. Foruzanmehr, L. Boulos, P. Y. Vuillaume, S. Elkoun, and M. Robert, *Cellulose*, doi:10.1007/s10570-016-1185-6, 1 (2017).
25. Z. Torabi and A. Mohammadi Nafchi, *J. Chem. Health Risks*, **3**, 33 (2013).
26. R. Kumar, M. K. Yakabu, and R. D. Anandjiwala, *Compos. Pt. A-Appl. Sci. Manuf.,* **41**, 1620 (2010).
27. F. Gauvin, C. Richard, and M. Robert, *Polym. Compos*. doi:10.1002/pc.24097 (2016).
28. G. Bogoeva-Gaceva, M. Avella, M. Malinconico, A. Buzarovska, A. Grozdanov, G. Gentile, and M. E. Errico, *Polym. Compos*., **28**, 98 (2007).
29. R. L. Reddy, V. S. Reddy, and G. A. Gupta, *Int. J. Emerg. Technol. Adv. Eng*., **3**, 76 (2013).
30. M. Baiardo, G. Frisoni, M. Scandola, M. Rimelen, D. Lips, K. Ruffieux, and E. Wintermantel, *J. Appl. Polym. Sci.*, **90**, 1731 (2003).
31. Mr. Foruzanmehr, P. Y. Vuillaume, S. Elkoun, and M. Robert, *Mater. Des*., **106**, 295 (2016).
32. K. Oksman, M. Skrifvars, and J.-F. Selin, *Compos. Sci. Technol.*, **63**, 1317 (2003).
33. C. D. Putnam, M. Hammel, G. L. Hura, and J. A. Tainer, *Q. Rev. Biophys.*, **40**, 191 (2007).
34. A. Espert, F. Vilaplana, and S. Karlsson, *Compos. Pt. A-Appl. Sci. Manuf.*, **35**, 1267 (2004).
35. A. G. Kikhney and D. I. Svergun, *FEBS Lett*., **589**, 2570 (2015).
36. M. Nyman and L. Fullmer in "Trends Polyoxometalates Research" (L. Ruhlmann and D. Schaming Eds.), pp.151-170, Nova Science Publishers Inc., 2015.
37. A. S. Herrmann, J. Nickel, and U. Riedel, *Polym. Degrad. Stabil*., **59**, 251 (1998).
38. C. L. Wu, M. Q. Zhang, M. Z. Rong, and K. Friedrich, *Compos. Sci. Technol*., **62**, 1327 (2002).
39. L. Boulos, M. Reza Foruzanmehr, A. Tagnit-Hamou, S. Elkoun, and M. Robert, *Surf. Coat. Technol*., doi:10.1016/j.biortech.2007.12.073 (2017).